Molecular Diversity
https://doi.org/10.1007/s11030-020-10071-9

ORIGINAL ARTICLE

Design, synthesis and evaluation of dihydrotriazine derivatives-bearing 5-aryloxypyrazole moieties as antibacterial agents

Tian-Yi Zhang[1] · Chun-Shi Li[2] · Ming-Yue Cui[2] · Xue-Qian Bai[1] · Jiang-Hui Chen[1,3] · Ze-Wen Song[1,3] · Bo Feng[1] · Xue-Kun Liu[4]

Received: 17 December 2019 / Accepted: 6 March 2020

Abstract

In the present investigation, a series of dihydrotriazine derivatives-bearing 5-aryloxypyrazole moieties were synthesized and their structures were confirmed by different spectral tools. The biological evaluation in vitro revealed that some of the target compounds exerted good antibacterial and antifungal activity in comparison with the reference drugs. Among these novel hybrids, compound **10d** showed the most potent activity with minimum inhibitory concentration values (MIC) of 0.5 µg/mL against *S. aureus* 4220, MRSA 3506 and *E. coli* 1924 strain. The cytotoxic activity of the compounds **6d**, **6m**, **10d** and **10g** was assessed in MCF-7 and HeLa cells. Growth kinetics study showed significant inhibition of bacterial growth when treated with different conc. of **10d**. In vitro enzyme study implied that compound **10d** exerted its antibacterial activity through DHFR inhibition. Moreover, significant inhibition of biofilm formation was observed in bacterial cells treated with MIC conc. of **10d** as visualized by SEM micrographs.

Tian-Yi Zhang and Chun-Shi Li have contributed equally to this work.

Electronic supplementary material The online version of this article (https://doi.org/10.1007/s11030-020-10071-9) contains supplementary material, which is available to authorized users.

✉ Tian-Yi Zhang
tianyizhang@126.com

✉ Bo Feng
jyfengb@126.com

✉ Xue-Kun Liu
liuxuekunth@126.com

[1] Jilin Medical University, Jilin 132013, People's Republic of China

[2] The Third People's Hospital of Dalian, Dalian 116000, People's Republic of China

[3] Department of Pharmacy, Yanbian University, Yanji 133002, People's Republic of China

[4] School of Pharmacy Medicine, Tonghua Normal University, Tonghua 134002, Jilin Province, People's Republic of China

Published online: 14 March 2020

Graphic abstract

Twenty-nine target compounds were designed, synthesized and evaluated in terms of their antibacterial and antifungal activities.

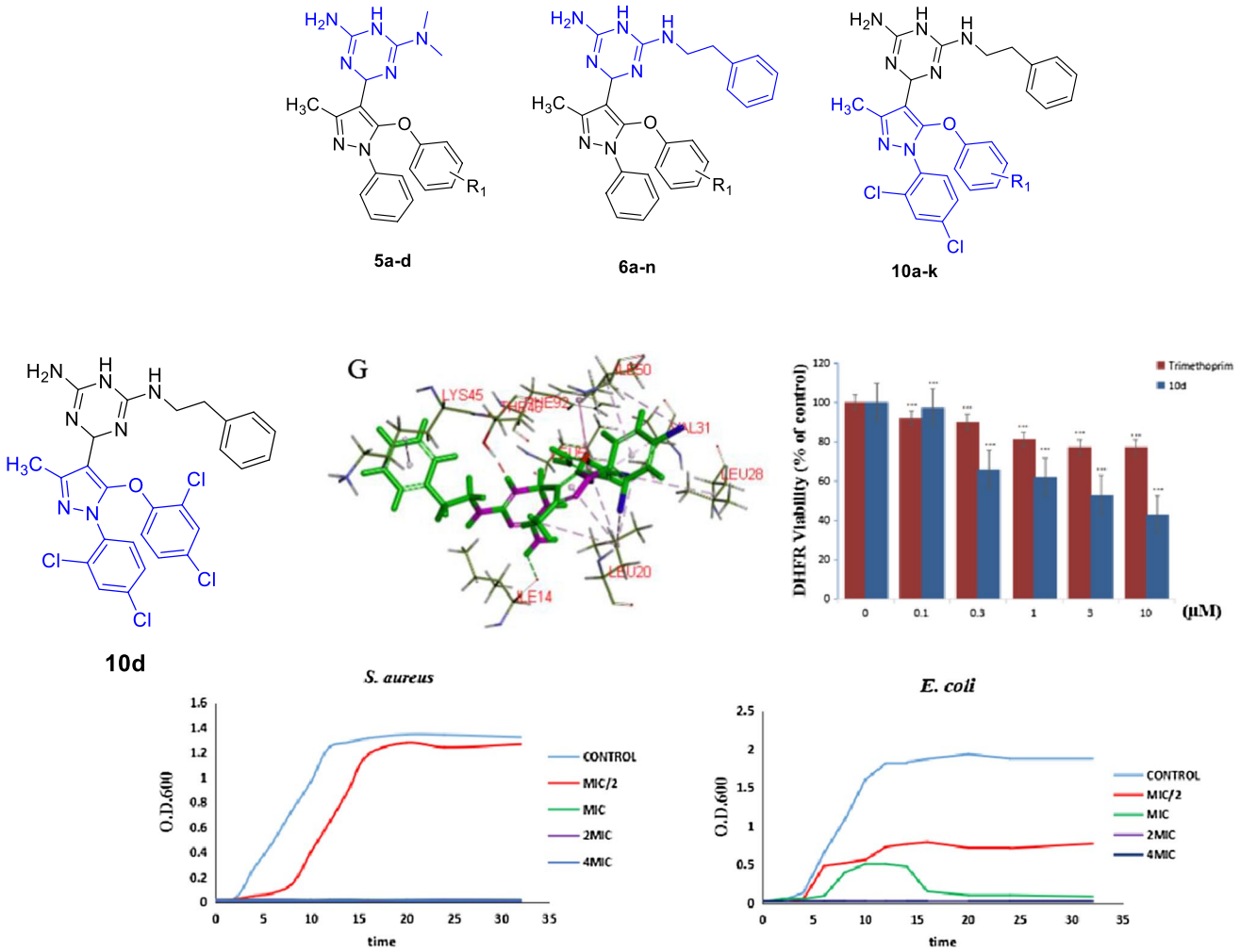

Keywords 5-Aryloxypyrazole · Dihydrotriazine · Antibacterial activity · Growth kinetics · DHFR inhibition

Introduction

Antimicrobial resistance (AMR) is a complex global health issue increasingly accelerated by selective pressure resulting from the use and misuse of antimicrobial agents in humans and animals [1]. The CDC currently estimates that antibiotic-resistant infections are responsible for at least 2 million illnesses and 23,000 deaths each year in the USA, with direct societal costs as high as $20 billion [2]. Compounding the issue of antibiotic resistance is the fact that very few new drugs have been approved to treat Gram-negative infections in recent decades, and the majority of these have come from well-known classes of drugs discovered half a century ago [3]. Therefore, discovery of novel classes of antibiotics that are effective against a broad range of bacteria, including those which have developed resistance to known drugs, has become an urgent challenge [4].

In the quest for new antibacterial agents, several heterocyclic scaffolds have been explored. Among them, pyrazoles represent a key structural motif in heterocyclic chemistry and occupy a significant position in medicinal and pesticide chemistry because of their capability to exhibit a wide range of biological activities, including antibacterial [5, 6], anti-inflammatory [7] and fungistatic [8]. The use of pyrazole derivatives as potential antimicrobial agents has received considerable attention following the discovery of the natural pyrazole C-glycoside, pyrazofurin that demonstrated a broad spectrum of antimicrobial activity [9]. Furthermore,

dihydrofolate reductase (DHFR), a key enzyme in the folate pathway, is responsible for reducing dihydrofolic acid to tetrahydrofolic acid. Tetrahydrofolate is involved in one carbon transfer reactions that lead to the biosynthesis of nucleic acids and amino acids. Thus, the inhibition of DHFR is able to arrest cell growth by depleting the cellular pool of DNA, RNA and protein synthesis precursors [10, 11]. DHFR has been recognized as a validated drug target for antibacterial agents [12].

The design of the presented set of compounds was based on our previous rhodanine derivatives which had more potent inhibitory activities against Gram-positive bacteria, as exemplified by compounds **A** and **B** (MIC = 2 μg/mL and 16 μg/mL, respectively) (Fig. 1) [13, 14]. Unfortunately, compounds belonging to this series did not show any bacteriostatic activity against Gram-negative bacteria. In contrast, our previous work indicated that compounds **C** and **D**, the dihydrotriazine derivatives containing pyrazole or quinoline moieties, had strong antimicrobial activities against many microorganisms such as Gram-negative, Gram-positive bacteria and fungi, including some clinically isolated drug-resistance microorganisms (Fig. 1) [15, 16]. In the present study, by use of compounds **A**–**D** as a starting template, we hypothesized that combining the structural features of 5-aryloxypyrazole and dihydrotriazine moieties could potentially have beneficial effect on the antibacterial activity (Fig. 2). The synthesized compounds were characterized and tested for their in vitro antibacterial activity. In addition, their structure–activity relationships, cytotoxicity and preliminary antibacterial mechanism were studied.

Results and discussion

Chemistry

As shown in Scheme 1, ethyl acetoacetate was reacted with phenylhydrazine or 2,4-dichlorophenylhydrazine to afford 3-methyl-1-phenyl-1*H*-pyrazol-5-ol (**2** or **7**). The intermediates (**2** or **7**) were treated with phosphorus oxychloride to

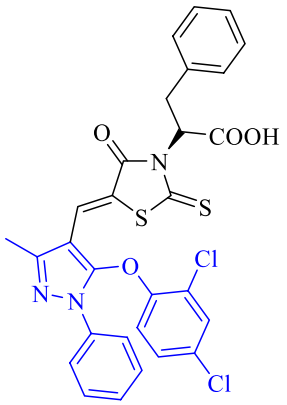

A **MIC** = 2 μg/mL (*S. aureus*)

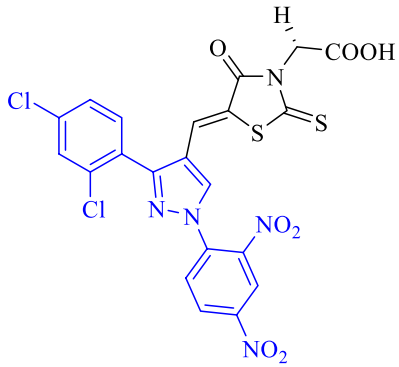

B **MIC** = 16 μg/mL (*S. aureus*)

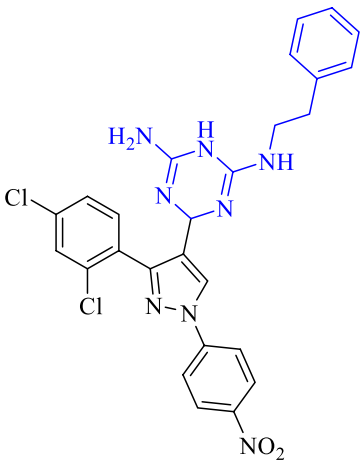

C **MIC** = 1 μg/mL (*S. aureus*)

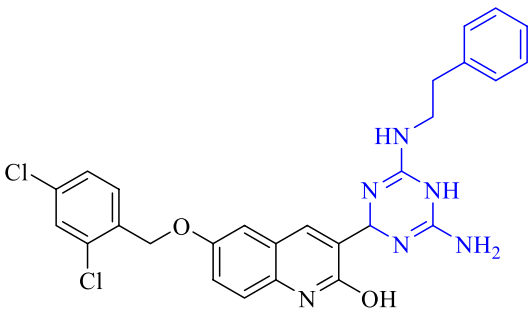

D **MIC** = 1 μg/mL (*S. aureus*)

Fig. 1 Chemical structures of some reported compounds and their MICs against *S. aureus*

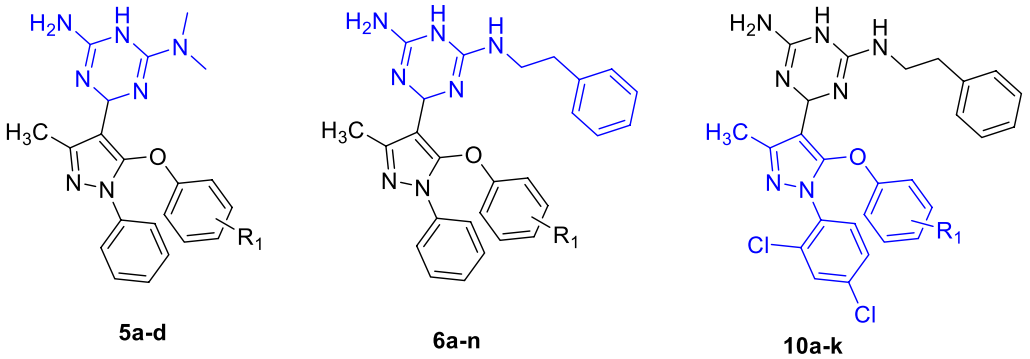

5a R_1= 2-Cl
5b R_1= 3-Cl
5c R_1= 4-Cl
5d R_1= 2,4-di-Cl
6a R_1= 2-Cl
6b R_1= 3-Cl
6c R_1= 4-Cl
6d R_1= 2,4-di-Cl
6e R_1= 3-Br
6f R_1= 4-Br
6g R_1= 4-F
6h R_1= 2-CH_3
6i R_1= 3-CH_3
6j R_1= 4-CH_3
6k R_1= 2,4-di-CH_3
6l R_1= 3-OCH_3
6m R_1= 3-CF_3
6n R_1= phenyl(3,4-fused)
10a R_1= 2-Cl
10b R_1= 3-Cl
10c R_1= 4-Cl
10d R_1= 2,4-di-Cl
10e R_1= 3-Br
10f R_1= 4-Br
10g R_1= 4-F
10h R_1= 4-CH_3
10i R_1= 2,4-di-CH_3
10j R_1= 3-CF_3
10k R_1= phenyl(3,4-fused)

Fig. 2 Design of target compounds based on the combination principles

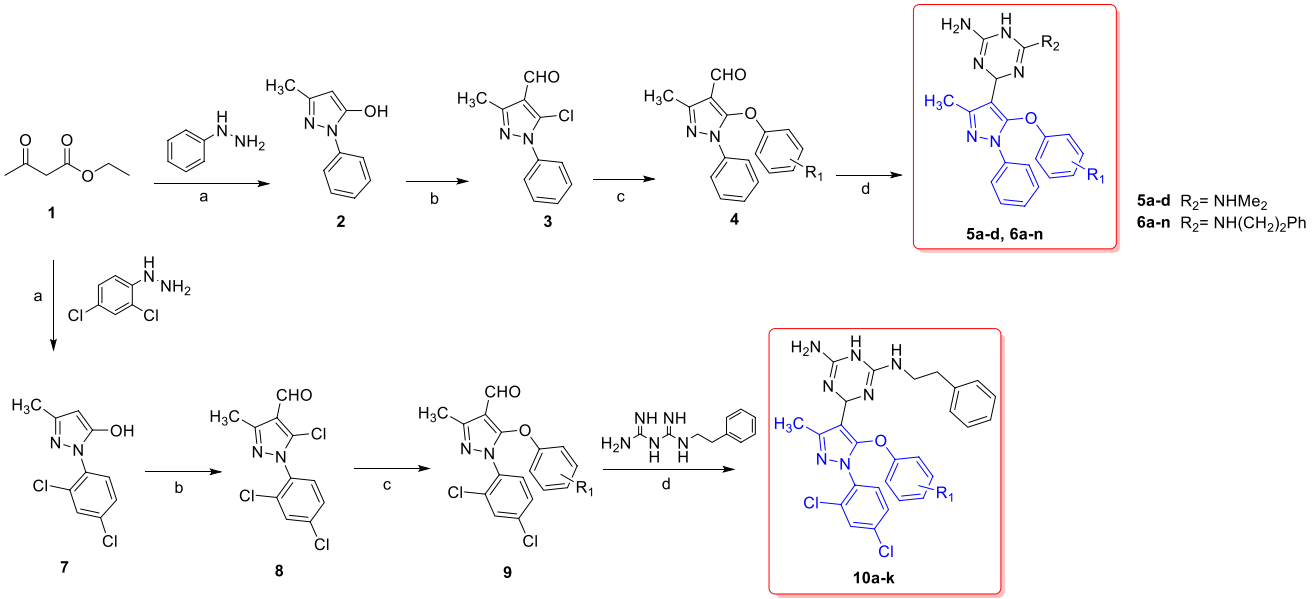

5a R_1= 2-Cl
5b R_1= 3-Cl
5c R_1= 4-Cl
5d R_1= 2,4-di-Cl
6a R_1= 2-Cl
6b R_1= 3-Cl
6c R_1= 4-Cl
6d R_1= 2,4-di-Cl
6e R_1= 3-Br
6f R_1= 4-Br
6g R_1= 4-F
6h R_1= 2-CH_3
6i R_1= 3-CH_3
6j R_1= 4-CH_3
6k R_1= 2,4-di-CH_3
6l R_1= 3-OCH_3
6m R_1= 3-CF_3
6n R_1= phenyl(3,4-fused)
10a R_1= 2-Cl
10b R_1= 3-Cl
10c R_1= 4-Cl
10d R_1= 2,4-di-Cl
10e R_1= 3-Br
10f R_1= 4-Br
10g R_1= 4-F
10h R_1= 4-CH_3
10i R_1= 2,4-di-CH_3
10j R_1= 3-CF_3
10k R_1= phenyl(3,4-fused)

Scheme 1 Synthetic scheme for the synthesis of the target compounds. Reagents and conditions: (a) phenylhydrazine or 2,4-dichlorophenylhydrazine, EtOH, *C*onc. HCl, 10% NaOH, 1 h, (b) $POCl_3$, DMF, 0 °C, 0.5 h, 80 °C, 3 h, (c) ROH, K_2CO_3, DMF, 80 °C, overnight, (d) metformin hydrochloride or phenformin hydrochloride, AcOH, 120 °C, 4–8 h

give 5-chloro-3-methyl-1-phenyl-1*H*-pyrazole-4-carbaldehyde (**3** or **8**), which was subsequently reacted with different substituted phenols to provide the intermediates (**4** or **9**). Then, a series of intermediates (**4** or **9**) were reacted with metformin hydrochloride or phenformin hydrochloride in acetic acid to generate the target compounds. Before biological evaluation, all target compounds were characterized via ^{1}H-NMR, ^{13}C-NMR and MS.

Antibacterial activity

Minimum inhibitory concentration (MIC) values of these compounds were calculated using standard methods. Antibacterial activity of the synthesized compounds was compared with trimethoprim, gatifloxacin, moxifloxacin and fluconazole. The compounds were screened against four Gram-positive strains (*S. aureus* 4220, QRSA CCARM 3505, MRSA CCARM 3506 and *S. mutans* 3289) and Gram-negative strains (*E. coli* 1924, *P. aeruginosa* 2742 and *S. typhimurium* 2421), as well as one fungus (*C. albicans* 7535), and the results are shown in Table 1. Against the Gram-positive *S. aureus* 4220, compounds (**10c**, **10d** and **10e**) had the highest activity, with an MIC value of 0.5 μg/mL, and this was slightly lower than gatifloxacin (MIC = 0.25 μg/mL) and moxifloxacin (MIC = 0.25 μg/mL). Against the Gram-negative *E. coli* 1924, compounds (**10a–f** and **10h–j)** were more potent than the positive controls gatifloxacin and moxifloxacin (MIC = 2 μg/mL), with an MIC of 0.5 μg/mL. Compounds **10b–f** and **10j** exhibited twofold more potent activity relative to trimethoprim (MIC = 32 μg/mL) with MIC values of 16 μg/mL against *P. aeruginosa* 2742, but weaker than that of gatifloxacin and moxifloxacin (MIC = 1 μg/mL). Regretfully, none of the compounds showed any inhibitory activity against the Gram-negative strain *S. typhimurium* 2421 (MICs > 64 μg/mL). Compounds (**10b–f** and **10h–k)** presented the highest activity with MIC values of 0.5 μg/mL against MRSA CCARM 3506, showed the twofold more potent activity relative to the standard drug moxifloxacin (MIC = 1 μg/mL), and eightfold more potent activity relative to trimethoprim (MIC = 4 μg/mL). For the fungus strains, compounds **10d** and **10 k** also displayed good potency, with an MIC of 2 μg/mL, which was slightly lower than that of fluconazole (MIC = 1 μg/mL).

Detailed structure–activity relationships (SAR) analysis on the dihydrotriazine and 5-aryloxypyrazole moieties revealed several structural features that are crucial to maintain the antibacterial activity. In general, both the position and the number of 2,4-di-Cl atom at the N^1 position of the pyrazole ring play a very important role in the antibacterial potency, as exemplified by the compounds in series **10**. Furthermore, no clear structure–activity relationships were observed, indicating that the antibacterial activity was not significantly affected by the position or physicochemical properties of the different substituents on the phenyl ring. Bioisosteric replacements of a dimethyl group at the *N*-position of the dihydro-1,3,5-triazine ring weakened the antibacterial activity. Based on these results, we reasonably hypothesized that the phenethyl group of the dihydro-1,3,5-triazine ring is an important structural feature that gives rise to promising antibacterial activity.

Cytotoxicity assessment by MTT assay

The cytotoxicity is one of the most essential criteria to evaluate the potential of antimicrobial agents. In order to identify the safety profile, the highly active compounds **6d**, **6m**, **10d** and **10g** were further evaluated for their toxicities against human breast cancer cells (MCF-7) and human cervical cells (HeLa) line using the colorimetric cell proliferation MTT assay. As shown in Table 2, compound **6d** exhibited slightly weaker activity than **10d** against the different bacteria, in spite of its greater cytotoxicity than **10d**, comparably indicating that the antibacterial activities exhibited by dihydrotriazine derivatives were not due to the cytotoxic effects.

Molecular docking

Molecular docking is considered as one of the convenient and effective theoretical methods in binding studies [18]. The crystal structure data were obtained from the Protein Data Bank (PDB code: 3fra), which was representative target to investigate the antibacterial mechanism. The structures of **5d**, **6d** and **10d** were sketched in 2D and converted into 3D using the DS molecule editor (Fig. 3). Compound **5d** is bound into the active site, in which the benzene ring at the N^1 position of the pyrazole formed alkyl bond with Leu20. The 2,4-di-Cl-substituted phenyl ring of **5d** formed pi-alkyl bond with Phe92 and Ile14. Compound **6d** is bound into the active site where the thiazine N atom shows interaction with Thr46. The 2,4-di-Cl substituted phenyl ring of **5d** shows interaction with Phe92 and Leu5. The pyrazole formed alkyl bond with Leu20. The phenethyl N atom of **6d** shows interaction with Gln95. Compound **10d** is bound into the active site, in which the position of the di-Cl substituent on the benzene ring at the N^1 position of the pyrazole formed alkyl bond with Leu20. The most stable contacts observed in **10d** shared four key binding residues including Phe92, Leu5, Thr46 and Ile14. Furthermore, with respect to DHFR enzyme, the two compounds were docked with the active domain and also the results indicated that the binding mode of compound **10d** was better than compound **5d** (Fig. 3c, i). These molecular docking data provide certain theoretical support for experimental results and the next optimization.

Table 1 Antibacterial data as MIC[a] (μg/mL) for target compounds **5a–d**, **6a–n** and **10a–k**

	R_1	R_2	Gram-positive strains			Fungus			Gram-negative strains	
			S. aureus	QRSA	MRSA	*S. mutans*	*C. albicans*	*E. coli*	*P. aeruginosa*	*S. typhimurium*
			4220[b]	3505[c]	3506[d]	3289[e]	7535[f]	1924[g]	2742[h]	2421[i]
5a	2-Cl	$NHMe_2$	64	> 64	64	> 64	> 64	64	64	> 64
5b	3-Cl	$NHMe_2$	64	> 64	32	> 64	> 64	32	32	> 64
5c	4-Cl	$NHMe_2$	64	> 64	64	> 64	> 64	64	32	> 64
5d	2,4-di-Cl	$NHMe_2$	32	64	32	64	> 64	32	32	> 64
6a	2-Cl	$NH(CH_2)_2Ph$	2	16	2	8	16	4	32	> 64
6b	3-Cl	$NH(CH_2)_2Ph$	2	16	2	8	16	4	32	> 64
6c	4-Cl	$NH(CH_2)_2Ph$	2	16	2	4	16	2	64	> 64
6d	2,4-di-Cl	$NH(CH_2)_2Ph$	1	8	1	4	8	1	> 64	> 64
6e	3-Br	$NH(CH_2)_2Ph$	2	16	1	8	16	2	64	> 64
6f	4-Br	$NH(CH_2)_2Ph$	2	16	1	4	16	2	64	> 64
6g	4-F	$NH(CH_2)_2Ph$	4	32	4	16	64	4	64	> 64
6h	2-CH_3	$NH(CH_2)_2Ph$	4	32	2	8	64	4	> 64	> 64
6i	3-CH_3	$NH(CH_2)_2Ph$	4	64	2	16	32	4	64	> 64
6j	4-CH_3	$NH(CH_2)_2Ph$	4	32	2	8	32	2	64	> 64
6k	2,4-di-CH_3	$NH(CH_2)_2Ph$	2	32	1	4	32	2	64	> 64
6l	3-OCH_3	$NH(CH_2)_2Ph$	8	64	4	16	64	4	> 64	> 64
6m	3-CF_3	$NH(CH_2)_2Ph$	2	32	2	4	8	2	64	> 64
6n	Phenyl(3,4-fused)	$NH(CH_2)_2Ph$	1	32	1	4	8	1	64	> 64
10a	2-Cl	$NH(CH_2)_2Ph$	1	16	1	2	4	0.5	32	> 64
10b	3-Cl	$NH(CH_2)_2Ph$	1	8	0.5	2	4	0.5	16	> 64
10c	4-Cl	$NH(CH_2)_2Ph$	0.5	8	0.5	2	4	0.5	16	> 64
10d	2,4-di-Cl	$NH(CH_2)_2Ph$	0.5	8	0.5	1	2	0.5	16	> 64
10e	3-Br	$NH(CH_2)_2Ph$	0.5	8	0.5	2	4	0.5	16	> 64
10f	4-Br	$NH(CH_2)_2Ph$	1	8	0.5	1	4	0.5	16	> 64
10g	4-F	$NH(CH_2)_2Ph$	2	16	1	4	16	1	32	> 64
10h	4-CH_3	$NH(CH_2)_2Ph$	1	16	0.5	2	8	0.5	32	> 64
10i	2,4-di-CH_3	$NH(CH_2)_2Ph$	1	16	0.5	2	4	0.5	32	> 64
10j	3-CF_3	$NH(CH_2)_2Ph$	1	16	0.5	2	4	0.5	16	> 64
10k	Phenyl(3,4-fused)	$NH(CH_2)_2Ph$	1	16	0.5	2	2	1	32	> 64
Gatifloxacin			0.25	8	2	0.25	nd	2	1	0.5
Moxifloxacin			0.25	4	1	0.25	nd	2	1	0.5
Fluconazole			nd	nd	nd	nd	1	nd	nd	Nd
Trimethoprim			32	4	4	0.5	2	4	32	2

nd not determined

[a]MICs were determined by microbroth dilution method for microdilution plates

[b]*S. aureus* 4220

[c]QRSA 3505

[d]MRSA 3506

[e]*S. mutans* 3289

[f]*Candida albicans* 7535

[g]*E. coli* 1924

[h]*Pseudomonas aeruginosa* 2742

[i]*Salmonella typhimurium* 2421

Table 2 Antibacterial activity and cytotoxicity for **6d**, **6m**, **10d** and **10g**

	Test organisms	6d	6m	10d	10g
MIC (μmol/L)	*S. aureus* 4220	1.87	3.75	0.83	3.6
	MRSA 3506	1.87	3.75	0.83	1.81
IC_{50}^{a} (μmol/L)	MCF-7[b]	7.61	30.13	29.11	35.10
	HeLa[c]	2.32	14.30	22.02	15.68

[a]IC_{50} is defined as the concentration to inhibit the cell growth by 50%

[b]Human breast cancer cells

[c]Human cervical cells

Inhibition studies of compound 10d with DHFR

We assayed compounds **10d** (MIC of 0.5 μg/mL) and standard drugs (**trimethoprim**) against DHFR in order to confirm that the observed antibacterial activity was clearly influenced by this enzyme inhibition (Fig. 4). The results indicated that compound **10d** rendered a good inhibitory potency against the enzymes as compared to the standard inhibitors. Furthermore, at concentrations of 10 μmol/L, compound **10d** decreased DHFR activity by 43% compared with the negative control. The results suggested that the analogues were active antibacterial compounds inhibiting dihydrofolate reductase enzyme.

Growth kinetic studies

There is always a need to discover rapidly bactericidal agents to combat antibacterial resistance, and time–kill kinetics is an important method to judge the efficacy of investigational antimicrobial agents [17, 18]. Based on the DHFR inhibition as well as the antibacterial effect on sensitive/resistant bacterial strains, compound **10d** was evaluated for its effect on the growth of *S. aureus* bacterial strains. The results showed that **10d** exerted significant effect on the growth pattern of these strains and completely inhibited the growth of *S. aureus* even at sub-MIC values with a continuous lag-phase of 32 h. Furthermore, at 2MIC and 4MIC values, no growth was observed in case of *S. aureus* and *E. coli* even after 32 h of incubation. Therefore, it can be concluded that **10d** is bacteriostatic in nature and effectively arrests the bacterial growth (Fig. 5).

Assessment of biofilm formation

Bacterial biofilm, a complex bacterial lifestyle adaptation, provides a protection from environmental stresses

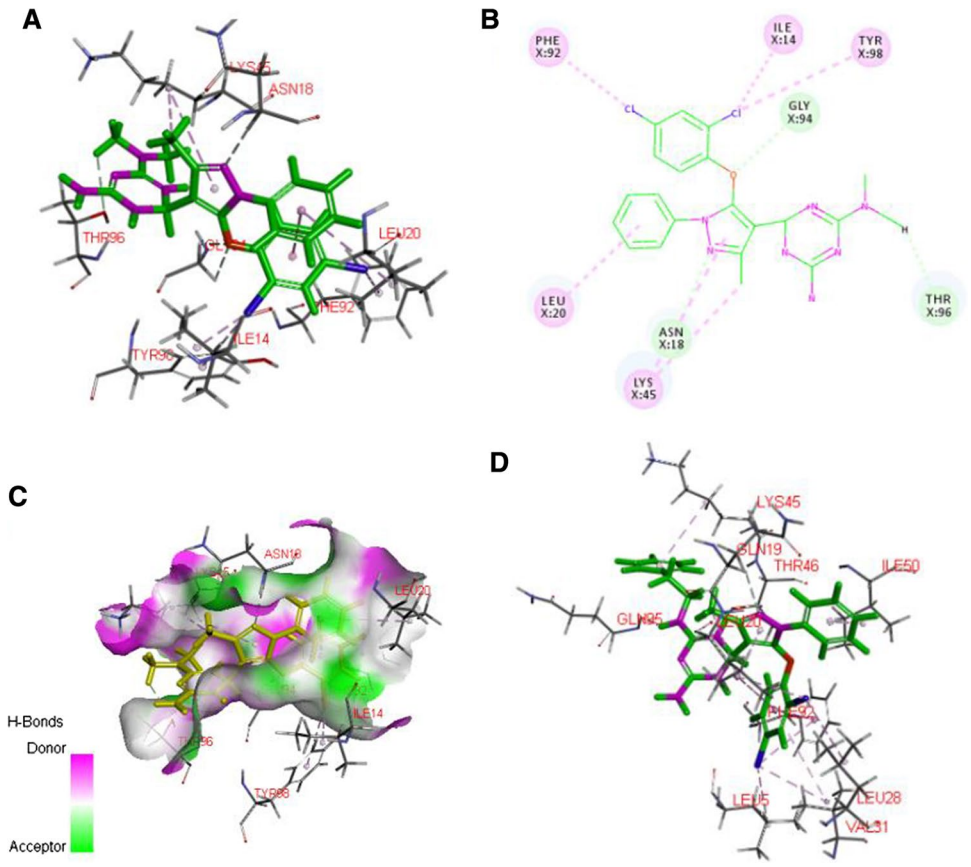

Fig. 3 **a** Three-dimensional conformation of compound **5d** docked in DHFR complex. **b** 2D molecular docking modeling of compound **5d** with 3fra. **c** Interaction of **5d** with DHFR inside the binding pocket. **d** Three-dimensional conformation of compound **6d** docked in DHFR complex. **e** 2D molecular docking modeling of compound **6d** with 3fra. **f** Interaction of **6d** with DHFR inside the binding pocket. **g** Three-dimensional conformation of compound **10d** docked in DHFR complex. **h** 2D molecular docking modeling of compound **10d** with 3fra. **i** Interaction of **10d** with DHFR inside the binding pocket

Fig. 3 (continued)

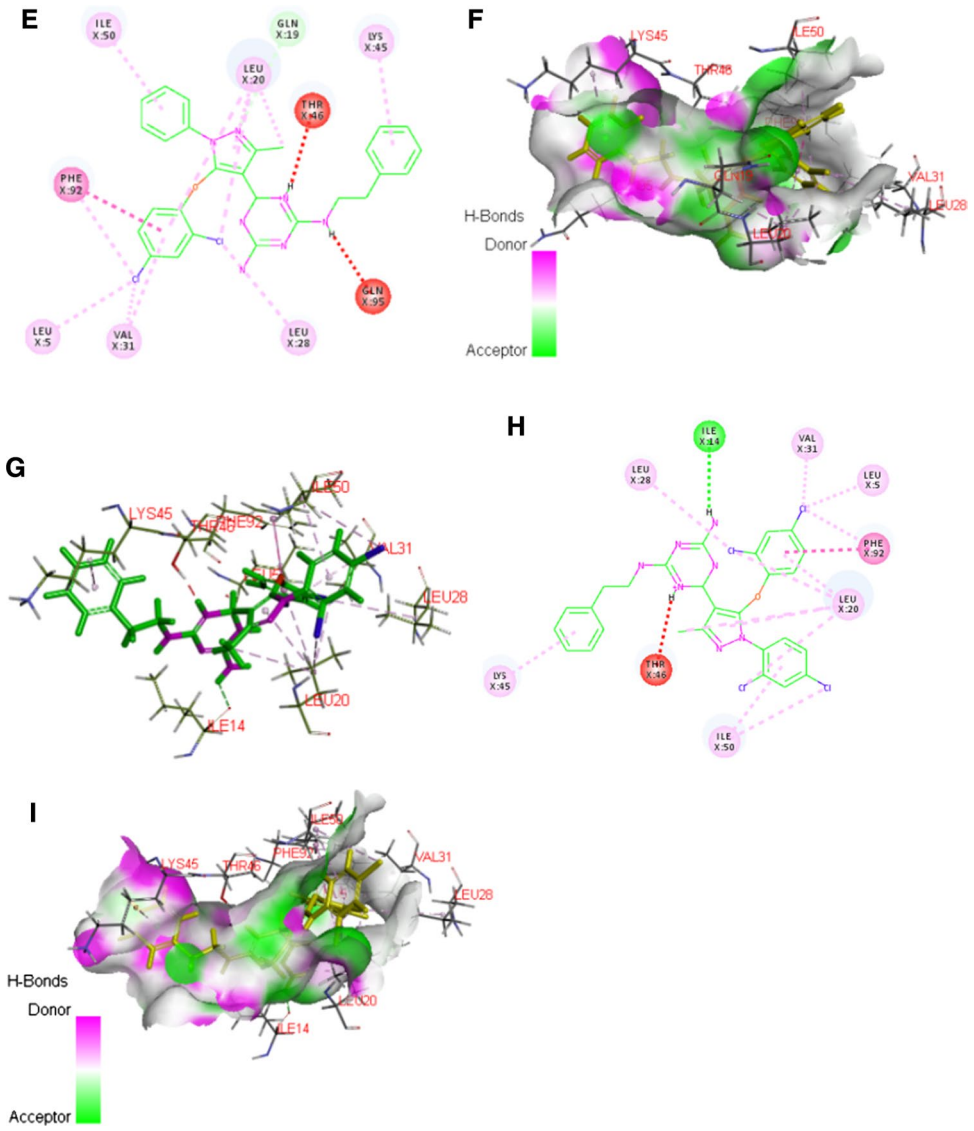

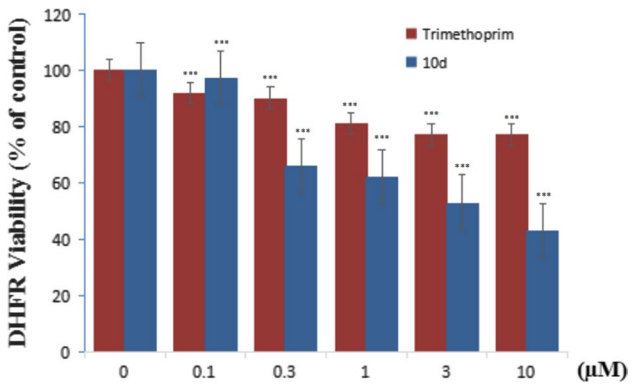

Fig. 4 Inhibition of DHFR activities of compounds **10d** and **trimethoprim**. Data are represented as the mean ± standard deviation of three independent experiments. ***$p < 0.05$, significant with respect to the control

[19]. When biofilms accompany bacterial infections, they make the infections extremely difficult to treat because bacterial cells in a biofilm exhibit stronger resistance to both the host immune system and antibiotic treatments [20]. Therefore, once biofilms have colonized the wound, the morbidity and mortality of skin–wound patients, as well as treatment cost, will greatly increase. To see the effect of lead inhibitor, SEM analysis was performed to visualize the effect of **10d** on biofilm formation using *S. aureus* strain. Significant inhibition of biofilm development was observed in *S. aureus* on treatment with MIC concentration (0.5 μg/mL) of compound **10d**. Clustering of cells which signifies the formation of biofilm was observed in untreated samples, while scattered cells with poor cell density were observed in treated cells. So, it can be concluded that the **10d** may have the potential to be an antibiofilm agent as well as an antibacterial agent (Fig. 6).

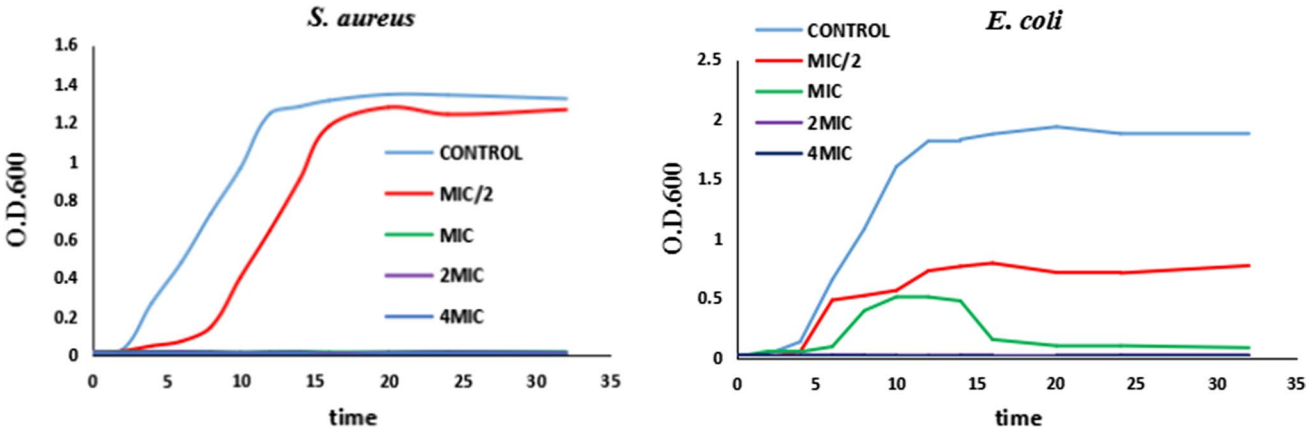

Fig. 5 Effect of different concentrations of compound **10d** on the growth kinetic studies

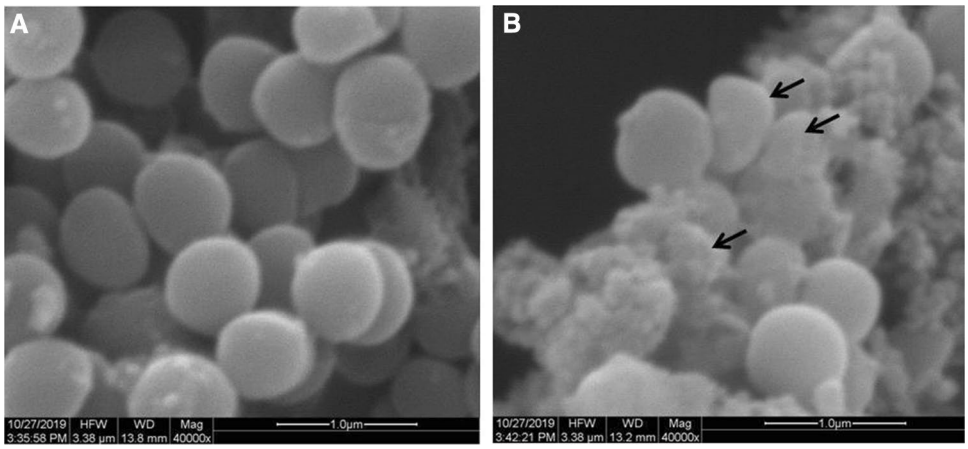

Fig. 6 Scanning electron microscopy of biofilm: **a** untreated, left; **b** treated with MIC concentration of compound **10d**, right

Conclusions

To summarize, three novel series of dihydrotriazine derivatives-bearing 5-aryloxypyrazole moieties were prepared via a convenient synthetic route and their antibacterial activity was evaluated. The structure–activity relationships were summarized which provided some important guidance for the development of antibacterial agents. Compound **10d** presented the most potent inhibitory activity against Gram-positive bacteria (*S. aureus* 4220, MRSA 3506) and Gram-negative bacteria (*E. coli* 1924), with minimum inhibitory concentration values of 0.5 µg/mL. Compound **10d** also inhibited the growth of various bacterial strains at different concentrations as signified by growth kinetics study. In vitro enzyme study implied that compound **10d** possibly displayed their antibacterial activity through DHFR protein inhibition. Furthermore, compound **10d** also inhibited the formation of biofilm in *S. aureus* as seen in SEM micrographs.

Materials and methods

General procedures

All commercially available reagents and solvents employed were used without further purification. All reactions were monitored by thin-layer chromatography (TLC) performed on silica gel plates. Melting points were determined in open capillaries and were uncorrected. Chemical shifts in ^{1}H NMR and ^{13}C NMR spectra are reported in parts per million (ppm) relative to tetramethylsilane (TMS). ^{1}H NMR and ^{13}C NMR spectra were performed on an AV-300 or AV-500 spectrometer (Bruker, Zurich, Switzerland) operating at 300 MHz for ^{1}H and 126 MHz for ^{13}C and using DMSO-d_6 as solvent. The following abbreviations were used to describe peak patterns: s = singlet, d = doublet, t = triplet, q = quadruplet, m = multiplet. Coupling constants (*J*) were expressed in hertz unit (Hz). Mass spectra were measured on an MALDI-TOF (Shimadzu, Japan).

General synthetic procedure for the key intermediates 2 and 7

To a stirred solution of acetylacetic ether (0.1 mol) and 70% ethanol (5.0 mL), the solution of phenylhydrazine (0.1 mol) with absolute alcohol (3.0 mL) was added dropwise at 45 °C, and the mixture was stirred for 20 min at this temperature. Cooled to 20 °C, concentrated hydrochloric acid (1.0 mL) was added dropwise and made to react for 2 h at 45 °C. Then, the PH value of mixture was adjusted to 7 using 10% NaOH solution, added 20 mL water and stirred for 1 h at the room temperature. The precipitated solid was filtered and washed with cold absolute alcohol to get a white solid (**2** and **7**).

General synthetic procedure for the key intermediates 3 and 8

To a cold, stirred solution of dimethylformamide (1 mmol) and phosphorous oxychloride (6 mmol) was added compound **2** (1 mmol). The reaction mixture was stirred at 80 °C for 3 h, cooled to room temperature and poured into ice–cold water whereupon a solid separated out that was filtered, washed with excess of cold water and dried to afford a yellow solid (**3** and **8**).

General synthetic procedure for the key intermediates 4 and 9

To a solution of compound **3** (10 mmol) and K_2CO_3 (15 mmol) in dry dimethylformamide (10 mL), corresponding substituted phenols (11 mmol) were added and mixture was stirred overnight at 80 °C. After the completion of reaction, the mixture was poured into 100 mL ice–water and filtered to obtain a white solid. The resulting crude solid (**4** and **9**) was directly used in the next step without purification.

General synthetic procedure for the target compounds 5a–d, 6a–n and 10a–k

Synthesized intermediate compounds (**4** and **9**) (1 mmol) and metformin hydrochloride or phenformin hydrochloride (1 mmol) were refluxed in glacial acetic acid (10 mL) at 120 °C for 4–6 h. The whole processes of the reactions were traced by TLC and then removed solvent under reduced pressure. The crude products were purified by column chromatography (dichloromethane/methanol = 20:1).

6-(5-(2-Chlorophenoxy)-3-methyl-1-phenyl-1H-pyrazol-4-yl)-N²,N²-dimethyl-3,6-dihydro-1,3,5-triazine-2,4-diamine (5a) White solid, Yield 48%; m.p. 140–142 °C. ^{1}H NMR (300 MHz, DMSO-d_6) δ 8.77 (s, 1H, NH), 8.41 (s, 1H, NH_2), 7.49 (t, J = 8.5 Hz, 3H, Ar–H), 7.40 (t, J = 7.8 Hz, 2H, Ar–H), 7.29 (d, J = 7.2 Hz, 1H, Ar–H), 7.17 (d, J = 7.8 Hz, 1H, Ar–H), 7.06 (d, J = 7.8 Hz, 1H, Ar–H), 6.74 (d, J = 8.3 Hz, 1H, Ar–H), 5.78 (s, 1H, CH), 2.81 (s, 6H, CH_3), 2.36 (s, 3H, CH_3). ^{13}C NMR (126 MHz, DMSO-d_6) δ 157.63, 156.11, 151.82, 147.98, 145.09, 137.51, 130.93, 129.78, 128.95, 127.92, 125.07, 122.21, 121.42, 115.45, 108.60, 56.48, 55.84, 55.39, 37.09, 19.03, 13.79. MS (MALDI-TOF) *m/z* 424 (M + 1).

6-(5-(3-Chlorophenoxy)-3-methyl-1-phenyl-1H-pyrazol-4-yl)-N²,N²-dimethyl-3,6-dihydro-1,3,5-triazine-2,4-diamine (5b) White solid, Yield 46%; m.p. 138–140 °C. ^{1}H NMR (300 MHz, DMSO-d_6) δ 8.79 (s, 1H, NH), 8.41 (s, 1H, NH_2), 7.53 (d, J = 7.4 Hz, 2H, Ar–H), 7.42 (t, J = 7.8 Hz, 2H, Ar–H), 7.31 (s, 2H, Ar–H), 7.12 (d, J = 7.5 Hz, 1H, Ar–H), 6.98 (s, 1H, Ar–H), 6.86 (d, J = 8.3 Hz, 1H, Ar–H), 5.76 (s, 1H, CH), 2.82 (s, 6H, CH_3), 2.36 (s, 3H, CH_3). ^{13}C NMR (126 MHz, DMSO-d_6) δ 157.73, 157.18, 156.00, 148.07, 145.48, 137.54, 134.38, 131.78, 129.88, 127.89, 124.13, 122.38, 115.89, 114.43, 108.05, 56.48, 55.84, 55.39, 37.05, 19.02, 13.81. MS (MALDI-TOF) *m/z* 424 (M + 1).

6-(5-(4-Chlorophenoxy)-3-methyl-1-phenyl-1H-pyrazol-4-yl)-N²,N²-dimethyl-3,6-dihydro-1,3,5-triazine-2,4-diamine (5c) White solid, Yield 45%; m.p. 141–143 °C. ^{1}H NMR (300 MHz, DMSO-d_6) δ 8.82 (s, 1H, NH), 8.41 (s, 1H, NH_2), 7.52 (d, J = 7.4 Hz, 2H, Ar–H), 7.41 (t, J = 7.8 Hz, 2H, Ar–H), 7.32 (t, J = 9.2 Hz, 3H, Ar–H), 6.93 (d, J = 9.0 Hz, 2H, Ar–H), 5.73 (s, 1H, CH), 2.83 (s, 6H, CH_3), 2.35 (s, 3H, CH_3). ^{13}C NMR (126 MHz, DMSO-d_6) δ 157.76, 156.11, 155.38, 148.03, 145.80, 137.56, 130.14, 129.85, 127.8, 122.41, 117.44, 107.85, 56.48, 55.86, 55.39, 37.08, 19.03, 13.85. MS (MALDI-TOF) *m/z* 424 (M + 1).

6-(5-(2,4-Dichlorophenoxy)-3-methyl-1-phenyl-1H-pyrazol-4-yl)-N²,N²-dimethyl-3,6-dihydro-1,3,5-triazine-2,4-diamine (5d) White solid, Yield 45%; m.p. 152–154 °C. ^{1}H NMR (300 MHz, DMSO-d_6) δ 8.79 (s, 1H, NH), 8.47 (s, 1H, NH_2), 7.66 (d, J = 2.5 Hz, 1H, Ar–H), 7.51–7.39 (m, 4H, Ar–H), 7.29 (dd, J = 14.6, 7.9 Hz, 2H, Ar–H), 6.76 (d, J = 8.9 Hz, 1H, Ar–H), 5.80 (s, 1H, CH), 2.85 (s, 6H, CH_3), 2.36 (s, 3H, CH_3). ^{13}C NMR (126 MHz, DMSO-d_6) δ 157.57, 156.06, 150.94, 148.05, 144.74, 137.35, 130.30, 129.86, 128.83, 128.13, 122.61, 122.33, 116.78, 108.74, 56.48, 55.78, 55.39, 37.11, 19.03, 13.73. MS (MALDI-TOF) *m/z* 458 (M + 1).

6-(5-(2-Chlorophenoxy)-3-methyl-1-phenyl-1H-pyrazol-4-yl)-N²-phenethyl-3,6-dihydro-1,3,5-triazine-2,4-diamine (6a) White solid, Yield 52%; m.p.

101–103 °C. ^{1}H NMR (300 MHz, DMSO-d_6) δ 8.78 (s, 1H, NH), 8.69 (s, 1H, NH), 8.48 (s, 1H, NH_2), 7.89 (s, 1H, NH_2), 7.50 (d, J = 7.5 Hz, 2H, Ar–H), 7.42 (dd, J = 15.3, 7.9 Hz, 3H, Ar–H), 7.32–7.26 (m, 3H, Ar–H), 7.19 (dd, J = 14.7, 7.2 Hz, 4H, Ar–H), 7.05 (dd, J = 10.8, 4.5 Hz, 1H, Ar–H), 6.81 (t, J = 13.4 Hz, 1H, Ar–H), 5.73 (s, 1H, CH), 2.71 (t, J = 7.2 Hz, 2H, CH_2), 2.51–2.48 (m, 2H, CH_2), 2.32 (s, 3H, CH_3). ^{13}C NMR (126 MHz, DMSO-d_6) δ 158.22, 157.13, 151.82, 147.90, 145.53, 139.34, 137.45, 131.03, 129.80, 129.15, 128.81, 128.01, 126.73, 125.23, 122.33, 121.51, 115.69, 107.94, 56.49, 55.39, 41.90, 35.58, 19.03, 13.80. MS (MALDI-TOF) m/z 500 (M + 1).

6-(5-(3-Chlorophenoxy)-3-methyl-1-phenyl-1H-pyrazol-4-yl)-N²-phenethyl-3,6-dihydro-1,3,5-triazine-2,4-diamine (6b) White solid, Yield 50%; m.p. 79–81 °C. ^{1}H NMR (300 MHz, DMSO-d_6) δ 8.77 (s, 1H, NH), 8.68 (s, 1H, NH), 8.46 (s, 1H, NH_2), 7.89 (s, 1H, NH_2), 7.51 (d, J = 7.6 Hz, 2H, Ar–H), 7.42 (t, J = 7.8 Hz, 3H, Ar–H), 7.33–7.25 (m, 4H, Ar–H), 7.22 (d, J = 6.6 Hz, 2H, Ar–H), 7.11 (d, J = 7.9 Hz, 1H, Ar–H), 7.02 (s, 1H, Ar–H), 6.85 (s, 1H, Ar–H), 5.74 (s, 1H, CH), 2.72 (dd, J = 8.6, 5.3 Hz, 2H, CH_2), 2.50 (d, J = 1.7 Hz, 2H, CH_2), 2.32 (s, 3H, CH_3). ^{13}C NMR (126 MHz, DMSO-d_6) δ 158.31, 157.15, 147.94, 145.67, 139.34, 137.50, 134.46, 131.92, 129.88, 129.16, 128.80, 127.93, 126.72, 124.24, 122.46, 116.35, 114.30, 107.52, 56.48, 55.40, 41.91, 35.61, 19.03, 13.81. MS (MALDI-TOF) m/z 500 (M + 1).

6-(5-(4-Chlorophenoxy)-3-methyl-1-phenyl-1H-pyrazol-4-yl)-N²-phenethyl-3,6-dihydro-1,3,5-triazine-2,4-diamine (6c) White solid, Yield 50%; m.p. 87–88 °C. ^{1}H NMR (300 MHz, DMSO-d_6) δ 8.78 (s, 1H, NH), 8.71 (s, 1H, NH), 8.50 (s, 1H, NH_2), 7.88 (s, 1H, NH_2), 7.51 (d, J = 7.5 Hz, 2H, Ar–H), 7.42 (t, J = 7.8 Hz, 2H, Ar–H), 7.35–7.27 (m, 5H, Ar–H), 7.22 (d, J = 7.2 Hz, 3H, Ar–H), 6.95 (d, J = 7.8 Hz, 2H, Ar–H), 5.70 (s, 1H, CH), 2.72 (dd, J = 8.9, 5.3 Hz, 2H, CH_2), 2.52–2.49 (m, 2H, CH_2), 2.31 (s, 3H, CH_3). ^{13}C NMR (126 MHz, DMSO-d_6) δ 158.26, 157.10, 155.40, 147.92, 145.97, 139.34, 137.51, 130.31, 129.87, 129.15, 128.81, 127.91, 126.73, 122.46, 117.56, 107.38, 56.49, 55.41, 41.90, 35.62, 19.03, 13.80. MS (MALDI-TOF) m/z 500 (M + 1).

6-(5-(2,4-Dichlorophenoxy)-3-methyl-1-phenyl-1H-pyrazol-4-yl)-N²-phenethyl-3,6-dihydro-1,3,5-triazine-2,4-diamine (6d) White solid, Yield 48%; m.p. 108–110 °C. ^{1}H NMR (300 MHz, DMSO-d_6) δ 8.79 (s, 1H, NH), 8.73 (s, 1H, NH), 8.52 (s, 1H, NH_2), 7.90 (s, 1H, NH_2), 7.66 (d, J = 2.5 Hz, 1H, Ar–H), 7.52–7.39 (m, 5H, Ar–H), 7.34–7.27 (m, 3H, Ar–H), 7.26–7.21 (m, 3H, Ar–H), 6.79 (d, J = 9.0 Hz, 1H, Ar–H), 5.77 (s, 1H, CH), 2.71 (t, J = 7.3 Hz, 2H, CH_2), 2.52–2.49 (m, 2H, CH_2), 2.32 (s, 3H, CH_3). ^{13}C NMR (126 MHz, DMSO-d_6) δ 158.12, 157.00, 150.96, 147.95, 145.04, 139.31, 137.30, 130.38, 129.88, 129.12, 128.82, 128.21, 126.73, 122.68, 122.42, 117.01, 108.27, 56.49, 55.39, 41.92, 35.57, 19.03, 13.69. MS (MALDI-TOF) m/z 534 (M + 1).

6-(5-(3-Bromophenoxy)-3-methyl-1-phenyl-1H-pyrazol-4-yl)-N²-phenethyl-3,6-dihydro-1,3,5-triazine-2,4-diamine (6e) White solid, Yield 48%; m.p. 95–96 °C. ^{1}H NMR (300 MHz, DMSO-d_6) δ 8.71 (s, 1H, NH), 8.62 (s, 1H, NH), 8.41 (s, 1H, NH_2), 7.89 (s, 1H, NH_2), 7.51 (d, J = 7.7 Hz, 2H, Ar–H), 7.42 (t, J = 7.8 Hz, 2H, Ar–H), 7.35–7.26 (m, 4H, Ar–H), 7.22 (d, J = 6.9 Hz, 4H, Ar–H), 7.14 (s, 1H, Ar–H), 6.92 (d, J = 26.0 Hz, 1H, Ar–H), 5.71 (d, J = 17.8 Hz, 1H, CH), 2.72 (t, J = 7.3 Hz, 2H, CH_2), 2.51 (d, J = 1.7 Hz, 2H, CH_2), 2.31 (s, 3H, CH_3). ^{13}C NMR (126 MHz, DMSO-d_6) δ 158.27, 157.15, 147.92, 145.66, 139.34, 137.51, 132.20, 129.88, 129.16, 128.81, 127.94, 127.13, 126.72, 122.68, 122.57, 119.13, 114.64, 107.51, 56.49, 55.41, 41.92, 35.61, 19.03, 13.80. MS (MALDI-TOF) m/z 544 (M + 1).

6-(5-(4-Bromophenoxy)-3-methyl-1-phenyl-1H-pyrazol-4-yl)-N²-phenethyl-3,6-dihydro-1,3,5-triazine-2,4-diamine (6f) White solid, Yield 50%; m.p. 101–102 °C. ^{1}H NMR (300 MHz, DMSO-d_6) δ 8.73 (s, 1H, NH), 8.65 (s, 1H, NH), 8.44 (s, 1H, NH_2), 7.88 (s, 1H, NH_2), 7.51 (d, J = 7.5 Hz, 2H, Ar–H), 7.47–7.39 (m, 4H, Ar–H), 7.34–7.27 (m, 3H, Ar–H), 7.22 (d, J = 7.1 Hz, 3H, Ar–H), 6.89 (d, J = 8.1 Hz, 2H, Ar–H), 5.71 (s, 1H, CH), 2.72 (t, J = 7.1 Hz, 2H, CH_2), 2.50 (d, J = 1.7 Hz, 2H, CH_2), 2.30 (s, 3H, CH_3). ^{13}C NMR (126 MHz, DMSO-d_6) δ 158.29, 157.18, 155.88, 147.92, 145.87, 139.33, 137.50, 133.23, 129.87, 129.16, 128.80, 127.91, 126.72, 122.45, 117.98, 115.81, 107.41, 56.49, 55.42, 41.91, 35.63, 19.03, 13.81. MS (MALDI-TOF) m/z 544 (M + 1).

6-(5-(4-Fluorophenoxy)-3-methyl-1-phenyl-1H-pyrazol-4-yl)-N²-phenethyl-3,6-dihydro-1,3,5-triazine-2,4-diamine (6g) White solid, Yield 50%; m.p. 87–89 °C. ^{1}H NMR (300 MHz, DMSO-d_6) δ 8.72 (s, 1H, NH_2), 8.64 (s, 1H, NH), 8.43 (s, 1H, NH_2), 7.88 (s, 1H, NH_2), 7.52 (d, J = 7.5 Hz, 2H, Ar–H), 7.42 (dd, J = 10.4, 5.2 Hz, 2H, Ar–H), 7.34–7.26 (m, 3H, Ar–H), 7.22 (d, J = 7.0 Hz, 3H, Ar–H), 7.11 (dd, J = 11.9, 5.5 Hz, 2H, Ar–H), 6.96 (s, 2H, Ar–H), 5.69 (s, 1H, CH), 2.74 (d, J = 6.9 Hz, 2H, CH_2), 2.51 (d, J = 1.8 Hz, 2H, CH_2), 2.30 (s, 3H, CH_3). ^{13}C NMR (126 MHz, DMSO-d_6) δ 13C NMR (126 MHz, DMSO) δ 159.42, 158.32, 157.52, 157.26, 152.78, 147.90, 146.55, 139.34, 137.59, 129.83, 129.16, 128.81, 127.86, 126.73, 122.50, 117.43, 116.97, 116.87, 116.72, 107.00, 56.49, 55.46, 41.90, 35.63, 19.03, 13.85. MS (MALDI-TOF) m/z 484 (M + 1).

6-(3-Methyl-1-phenyl-5-(o-tolyloxy)-1H-pyrazol-4-yl)-N²-phenethyl-3,6-dihydro-1,3,5-triazine-2,4-diamine (6h) White solid, Yield 46%; m.p. 87–89 °C. ^{1}H NMR (300 MHz, DMSO-d_6) δ 8.72 (s, 1H, NH), 8.63 (s, 1H, NH), 8.43 (s, 1H, NH_2), 7.82 (s, 1H, NH_2), 7.48 (s, 2H, Ar–H), 7.45–7.37 (m, 2H, Ar–H), 7.28 (s, 3H, Ar–H), 7.21 (s, 4H, Ar–H), 7.03 (s, 1H, Ar–H), 6.93 (s, 1H, Ar–H), 6.57 (s, 1H, Ar–H), 5.65 (s, 1H, CH), 2.68 (s, 2H, CH_2), 2.51 (s, 2H, CH_2), 2.30 (d, J = 3.2 Hz, 6H, CH_3). ^{13}C NMR (126 MHz, DMSO-d_6) δ 158.29, 157.18, 154.91, 147.83, 146.49, 139.34, 137.75, 131.70, 129.75, 129.14, 128.80, 127.84, 126.71, 126.14, 123.72, 122.33, 113.28, 107.20, 56.49, 55.47, 41.88, 35.57, 19.03, 16.19, 13.84. MS (MALDI-TOF) *m/z* 480 (M + 1).

6-(3-Methyl-1-phenyl-5-(m-tolyloxy)-1H-pyrazol-4-yl)-N²-phenethyl-3,6-dihydro-1,3,5-triazine-2,4-diamine (6i) White solid, Yield 46%; m.p. 81–83 °C. ^{1}H NMR (300 MHz, DMSO-d_6) δ 8.71 (s, 1H, NH), 8.62 (s, 1H, NH), 8.39 (s, 1H, NH_2), 7.88 (s, 1H, NH_2), 7.52 (d, J = 7.5 Hz, 2H, Ar–H), 7.42 (t, J = 7.8 Hz, 2H, Ar–H), 7.34–7.27 (m, 3H, Ar–H), 7.26–7.18 (m, 3H, Ar–H), 7.14 (d, J = 7.8 Hz, 1H, Ar–H), 6.87 (d, J = 7.3 Hz, 1H, Ar–H), 6.76 (s, 2H, Ar–H), 5.64 (s, 1H, CH), 2.72 (s, 2H, CH_2), 2.50 (d, J = 1.7 Hz, 2H, CH_2), 2.30 (s, 3H, CH_3), 2.24 (s, 3H, CH_3). ^{13}C NMR (126 MHz, DMSO-d_6) δ 158.41, 157.34, 156.67, 147.90, 146.51, 140.44, 139.34, 137.72, 130.24, 129.80, 129.16, 128.80, 127.74, 126.72, 124.87, 122.33, 116.05, 112.75, 106.76, 56.49, 55.49, 41.90, 35.64, 21.40, 19.03, 13.94. MS (MALDI-TOF) *m/z* 480 (M + 1).

6-(3-Methyl-1-phenyl-5-(p-tolyloxy)-1H-pyrazol-4-yl)-N²-phenethyl-3,6-dihydro-1,3,5-triazine-2,4-diamine (6j) White solid, Yield 48%; m.p. 88–89 °C. ^{1}H NMR (300 MHz, DMSO-d_6) δ 8.72 (s, 1H, NH), 8.63 (s, 1H, NH), 8.41 (s, 1H, NH_2), 7.88 (s, 1H, NH_2), 7.52 (d, J = 7.7 Hz, 2H, Ar–H), 7.41 (t, J = 7.9 Hz, 2H, Ar–H), 7.28 (s, 3H, Ar–H), 7.23 (s, 3H, Ar–H), 7.08 (d, J = 8.4 Hz, 2H, Ar–H), 6.84 (s, 2H, Ar–H), 5.63 (s, 1H, CH), 2.73 (s, 2H, CH_2), 2.51 (d, J = 1.7 Hz, 2H, CH_2), 2.30 (s, 3H, CH_3), 2.19 (s, 3H, CH_3). ^{13}C NMR (126 MHz, DMSO-d_6) δ 158.44, 157.37, 154.65, 147.87, 146.63, 139.35, 137.71, 133.04, 130.86, 129.79, 129.15, 128.80, 127.71, 126.72, 122.29, 115.43, 106.85, 56.49, 55.48, 41.91, 35.64, 20.54, 19.03, 13.96. MS (MALDI-TOF) *m/z* 480 (M + 1).

6-(5-(2,4-Dimethylphenoxy)-3-methyl-1-phenyl-1H-pyrazol-4-yl)-N²-phenethyl-3,6-dihydro-1,3,5-triazine-2,4-diamine (6 k) White solid, Yield 52%; m.p. 98–100 °C. ^{1}H NMR (300 MHz, DMSO-d_6) δ 8.67 (s, 1H, NH), 8.58 (s, 1H, NH), 8.38 (s, 1H, NH_2), 7.83 (s, 1H, NH_2), 7.49 (d, J = 7.7 Hz, 2H, Ar–H), 7.41 (t, J = 7.8 Hz, 2H, Ar–H), 7.32–7.26 (m, 3H, Ar–H), 7.21 (t, J = 5.6 Hz, 3H, Ar–H), 6.99 (s, 1H, Ar–H), 6.82 (d, J = 7.6 Hz, 1H, Ar–H), 6.44 (d, J = 8.0 Hz, 1H, Ar–H), 5.63 (s, 1H, CH), 2.68 (s, 2H, CH_2), 2.51 (d, J = 1.8 Hz, 2H, CH_2), 2.30 (s, 3H, CH_3), 2.26 (s, 3H, CH_3), 2.15 (s, 3H, CH_3). ^{13}C NMR (126 MHz, DMSO-d_6) δ 160.69, 157.81, 156.43, 154.33, 135.04, 133.30, 131.23, 121.25, 116.98, 110.89, 68.41, 59.20, 56.47, 37.48 (2C), 28.83, 28.19, 22.35, 14.38. MS (MALDI-TOF) *m/z* 494 (M + 1).

6-(5-(3-Methoxyphenoxy)-3-methyl-1-phenyl-1H-pyrazol-4-yl)-N²-phenethyl-3,6-dihydro-1,3,5-triazine-2,4-diamine (6l) Yellow solid, Yield 52%; m.p. 78–80 °C. ^{1}H NMR (300 MHz, DMSO-d_6) δ 8.66 (s, 1H, NH), 8.55 (s, 1H, NH), 8.34 (s, 1H, NH_2), 7.88 (s, 1H, NH_2), 7.53 (d, J = 7.6 Hz, 2H, Ar–H), 7.42 (t, J = 7.8 Hz, 2H, Ar–H), 7.33–7.27 (m, 3H, Ar–H), 7.19 (dd, J = 19.2, 7.4 Hz, 4H, Ar–H), 6.63 (d, J = 8.3 Hz, 1H, Ar–H), 6.48 (d, J = 12.9 Hz, 2H, Ar–H), 5.66 (s, 1H, CH), 3.69 (s, 3H, OCH_3), 2.73 (s, 2H, CH_2), 2.51 (d, J = 1.7 Hz, 2H, CH_2), 2.30 (s, 3H, CH_3). ^{13}C NMR (126 MHz, DMSO-d_6) δ 161.00, 158.37, 157.71, 157.30, 146.34, 139.34, 137.70, 131.06, 129.82, 129.16, 128.80, 127.77, 126.72, 122.35, 109.94, 107.45, 106.94, 102.17, 56.49, 55.65, 41.90, 35.62, 19.03, 13.93. MS (MALDI-TOF) *m/z* 496 (M + 1).

6-(3-Methyl-1-phenyl-5-(3-(trifluoromethyl)phenoxy)-1H-pyrazol-4-yl)-N²-phenethyl-3,6-dihydro-1,3,5-triazine-2,4-diamine (6m) White solid, Yield 50%; m.p. 87–89 °C. ^{1}H NMR (300 MHz, DMSO-d_6) δ 8.91 (s, 1H, NH), 8.66 (s, 1H, NH_2), 7.86 (s, 1H, Ar–H), 7.78 (d, J = 2.2 Hz, 1H, Ar–H), 7.63 (s, 1H, Ar–H), 7.47 (dd, J = 13.0, 4.5 Hz, 2H, Ar–H), 7.41 (d, J = 7.3 Hz, 2H, Ar–H), 7.33–7.25 (m, 2H, Ar–H), 7.21 (dd, J = 9.7, 4.5 Hz, 3H, Ar–H), 7.12 (s, 1H, Ar–H), 5.81 (s, 1H, CH), 2.68 (s, 2H, CH_2), 2.51–2.50 (m, 2H, CH_2), 2.31 (s, 3H, CH_3). ^{13}C NMR (126 MHz, DMSO-d_6) δ 158.28, 157.18, 156.60, 147.97, 145.63, 139.30, 137.45, 131.92, 131.10, 130.84, 129.85, 129.12, 128.79, 128.00, 126.71, 125.04, 122.87, 122.63, 120.82, 119.47, 113.28, 107.53, 56.48, 55.42, 41.86, 35.60, 19.02, 13.78. MS (MALDI-TOF) *m/z* 534 (M + 1).

6-(3-Methyl-5-(naphthalen-2-yloxy)-1-phenyl-1H-pyrazol-4-yl)-N²-phenethyl-3,6-dihydro-1,3,5-triazine-2,4-diamine (6n) Yellow solid, Yield 42%; m.p. 128–130 °C. ^{1}H NMR (300 MHz, DMSO-d_6) δ 8.77 (s, 1H, NH), 8.70 (s, 1H, NH), 8.43 (s, 1H, NH_2), 8.31 (d, J = 8.3 Hz, 1H, NH_2), 7.97–7.88 (m, 1H, Ar–H), 7.75 (s, 1H, Ar–H), 7.67–7.52 (m, 5H, Ar–H), 7.34–7.24 (m, 5H, Ar–H), 7.23–7.10 (m, 4H, Ar–H), 6.75 (t, J = 18.3 Hz, 1H, Ar–H), 5.67 (d, J = 19.2 Hz, 1H, CH), 3.17 (d, J = 22.0 Hz, 2H, CH_2), 2.58 (s, 2H, CH_2), 2.35 (s, 3H, CH_3). ^{13}C NMR (126 MHz, DMSO-d_6) δ 158.23, 157.16, 152.43, 147.98, 146.28, 139.26, 137.71, 134.64, 129.73, 129.09, 128.76, 128.08, 127.79, 127.52, 126.87,

126.55, 124.13, 123.58, 122.24, 121.50, 108.38, 107.49, 56.49, 55.46, 41.75, 35.41, 19.03, 13.88. MS (MALDI-TOF) *m/z* 516 (M + 1).

6-(5-(2-Chlorophenoxy)-1-(2,4-dichlorophenyl)-3-methyl-1H-pyrazol-4-yl)-N²-phenethyl--3,6-dihydro-1,3,5-triazine-2,4-diamine (10a) White solid, Yield 42%; m.p. 112–113 °C. ^{1}H NMR (300 MHz, DMSO-d_6) δ 8.76 (s, 1H, NH), 8.63 (s, 1H, NH), 8.44 (s, 1H, NH_2), 7.91 (s, 1H, NH_2), 7.80 (d, J = 2.2 Hz, 1H, Ar–H), 7.45 (dd, J = 8.5, 2.3 Hz, 1H, Ar–H), 7.40–7.34 (m, 2H, Ar–H), 7.33–7.26 (m, 2H, Ar–H), 7.21 (d, J = 7.6 Hz, 4H, Ar–H), 7.10–7.02 (m, 1H, Ar–H), 6.97 (d, J = 7.0 Hz, 1H, Ar–H), 5.79 (s, 1H, CH), 2.73 (d, J = 6.6 Hz, 2H, CH_2), 2.51 (d, J = 1.7 Hz, 2H, CH_2), 2.30 (s, 3H, CH_3). ^{13}C NMR (126 MHz, DMSO-d_6) δ 158.27, 157.24, 151.88, 148.42, 147.43, 139.31, 135.50, 133.38, 132.73, 131.26, 130.78, 130.24, 129.14, 128.72, 128.64–128.41, 126.72, 125.53, 121.88, 117.11, 106.82, 56.49, 55.38, 41.89, 35.58, 19.03, 13.86. MS (MALDI-TOF) *m/z* 568 (M + 1).

6-(5-(3-Chlorophenoxy)-1-(2,4-dichlorophenyl)-3-methyl-1H-pyrazol-4-yl)-N²-phenethyl--3,6-dihydro-1,3,5-triazine-2,4-diamine (10b) White solid, Yield 40%; m.p. 91–93 °C. ^{1}H NMR (300 MHz, DMSO-d_6) δ 8.70 (s, 1H, NH), 8.56 (s, 1H, NH), 8.37 (s, 1H, NH_2), 7.90 (s, 1H, NH_2), 7.81 (d, J = 2.2 Hz, 1H, Ar–H), 7.49 (dd, J = 8.5, 2.3 Hz, 1H, Ar–H), 7.41 (d, J = 8.3 Hz, 1H, Ar–H), 7.33–7.25 (m, 3H, Ar–H), 7.25–7.18 (m, 3H, Ar–H), 7.12 (d, J = 7.3 Hz, 1H, Ar–H), 6.89 (d, J = 20.3 Hz, 2H, Ar–H), 5.79 (s, 1H, CH), 2.72 (d, J = 7.0 Hz, 2H, CH_2), 2.51 (d, J = 1.8 Hz, 2H, CH_2), 2.30 (s, 3H, CH_3). ^{13}C NMR (126 MHz, DMSO-d_6) δ 158.24, 157.08, 156.86, 156.71, 148.93, 148.48, 147.88, 139.31, 135.44, 134.28, 133.58, 131.76, 131.26, 131.26, 130.35, 129.14, 128.82, 126.73, 124.47, 116.57, 115.05, 106.52, 56.48, 55.39, 41.88, 35.59, 19.03, 13.82. MS (MALDI-TOF) *m/z* 568 (M + 1).

6-(5-(4-Chlorophenoxy)-1-(2,4-dichlorophenyl)-3-methyl-1H-pyrazol-4-yl)-N²-phenethyl--3,6-dihydro-1,3,5-triazine-2,4-diamine (10c) White solid, Yield 42%; m.p. 108–110 °C. ^{1}H NMR (300 MHz, DMSO-d_6) δ 8.72 (s, 1H, NH), 8.58 (d, J = 21.4 Hz, 1H, NH), 8.42 (s, 1H, NH_2), 7.82 (d, J = 2.1 Hz, 1H, Ar–H), 7.50 (dd, J = 8.5, 2.2 Hz, 1H, Ar–H), 7.42 (d, J = 7.8 Hz, 2H, Ar–H), 7.29 (d, J = 8.5 Hz, 3H, Ar–H), 7.25–7.19 (m, 3H, Ar–H), 6.91 (d, J = 8.6 Hz, 2H, Ar–H), 5.74 (s, 1H, CH), 2.71 (t, J = 7.0 Hz, 2H, CH_2), 2.51 (d, J = 1.7 Hz, 2H, CH_2), 2.29 (s, 3H, CH_3). ^{13}C NMR (126 MHz, DMSO-d_6) δ 158.28, 157.21, 155.29, 148.53, 147.55, 139.32, 135.45, 133.66, 132.37, 131.34, 130.32, 130.12, 129.14, 128.81, 128.08, 126.73, 117.96, 106.22, 56.49, 55.39, 41.87, 35.60, 19.03, 13.84. MS (MALDI-TOF) *m/z* 568 (M + 1).

6-(5-(2,4-Dichlorophenoxy)-1-(2,4-dichlorophenyl)-3-methyl-1H-pyrazol-4-yl)-N²-phenethyl-3,6-dihydro-1,3,5-triazine-2,4-diamine (10d) White solid, Yield 42%; m.p. 119–120 °C. ^{1}H NMR (300 MHz, DMSO-d_6) δ 8.77 (s, 1H, NH), 8.66 (s, 1H, NH), 8.47 (s, 1H, NH_2), 7.91 (s, 1H, NH_2), 7.84 (d, J = 2.2 Hz, 1H, Ar–H), 7.58 (d, J = 2.5 Hz, 1H, Ar–H), 7.49 (dd, J = 8.5, 2.3 Hz, 1H, Ar–H), 7.39 (d, J = 8.7 Hz, 2H, Ar–H), 7.29 (d, J = 7.1 Hz, 2H, Ar–H), 7.25–7.19 (m, 3H, Ar–H), 7.00 (d, J = 9.0 Hz, 1H, Ar–H), 5.82 (s, 1H, CH), 2.72 (d, J = 6.2 Hz, 2H, CH_2), 2.51 (d, J = 1.8 Hz, 2H, CH_2), 2.30 (s, 3H, CH_3). ^{13}C NMR (126 MHz, DMSO-d_6) δ 158.21, 157.13, 151.01, 148.52, 146.89, 139.30, 135.68, 133.26, 132.71, 131.33, 130.24, 129.24, 128.67, 128.54, 126.73, 122.96, 118.26, 107.12, 56.48, 55.39, 41.89, 35.59, 19.03, 13.77. MS (MALDI-TOF) *m/z* 602 (M + 1).

6-(5-(3-Bromophenoxy)-1-(2,4-dichlorophenyl)-3-methyl-1H-pyrazol-4-yl)-N²-phenethyl-3,6-dihydro-1,3,5-triazine-2,4-diamine (10e) White solid, Yield 44%; m.p. 90–92 °C. ^{1}H NMR (300 MHz, DMSO-d_6) δ 8.85 (s, 1H, NH), 8.74 (s, 1H, NH), 8.59 (s, 1H, NH_2), 7.88 (s, 1H, NH_2), 7.81 (d, J = 2.2 Hz, 1H, Ar–H), 7.55 (s, 1H, Ar–H), 7.49 (dd, J = 8.5, 2.2 Hz, 1H, Ar–H), 7.40 (d, J = 8.3 Hz, 1H, Ar–H), 7.32–7.25 (m, 2H, Ar–H), 7.24–7.15 (m, 4H, Ar–H), 7.04 (s, 1H, Ar–H), 6.91 (s, 1H, Ar–H), 5.77 (s, 1H, CH), 2.77–2.66 (m, 2H, CH_2), 2.51 (d, J = 1.7 Hz, 2H, CH_2), 2.30 (s, 3H, CH_3). ^{13}C NMR (126 MHz, DMSO-d_6) δ 158.27, 157.09, 147.29, 135.43, 133.59, 132.15, 131.80, 131.52, 131.25, 130.35, 129.14, 128.80, 127.37, 126.72, 122.45, 119.39, 115.46, 56.49, 55.39, 41.89, 35.59, 22.38, 19.03, 13.82. MS (MALDI-TOF) *m/z* 612 (M + 1).

6-(5-(4-Bromophenoxy)-1-(2,4-dichlorophenyl)-3-methyl-1H-pyrazol-4-yl)-N²-phenethyl-3,6-dihydro-1,3,5-triazine-2,4-diamine (10f) White solid, Yield 40%; m.p. 105–107 °C. ^{1}H NMR (300 MHz, DMSO-d_6) δ 8.72 (s, 1H, NH), 8.58 (s, 1H, NH), 8.43 (s, 1H, NH_2), 7.89 (s, 1H, NH_2), 7.82 (d, J = 2.2 Hz, 1H, Ar–H), 7.50 (dd, J = 8.5, 2.3 Hz, 1H, Ar–H), 7.46–7.38 (m, 3H, Ar–H), 7.36–7.27 (m, 2H, Ar–H), 7.26–7.18 (m, 3H, Ar–H), 6.86 (d, J = 8.5 Hz, 2H, Ar–H), 5.74 (s, 1H, CH), 2.71 (t, J = 7.2 Hz, 2H, CH_2), 2.51 (d, J = 1.8 Hz, 2H, CH_2), 2.29 (s, 3H, CH_3). ^{13}C NMR (126 MHz, DMSO-d_6) δ 158.30, 157.20, 155.78, 148.55, 147.42, 139.32, 135.46, 133.64, 133.03, 132.38, 131.32, 130.33, 129.14, 128.81, 126.72, 118.34, 115.99, 106.26, 56.49, 55.39, 41.88, 35.61, 21.67, 19.03, 13.84. MS (MALDI-TOF) *m/z* 612 (M + 1).

6-(1-(2,4-Dichlorophenyl)-5-(4-fluorophenoxy)-3-methyl-1H-pyrazol-4-yl)-N²-phenethyl-3,6-dihydro-1,3,5-triazine-2,4-diamine (10g) White solid, Yield 40%; m.p. 103–104 °C. ^{1}H NMR (300 MHz, DMSO-d_6) δ 8.85 (s, 1H,

NH), 8.61 (s, 1H, NH), 7.81 (d, $J = 2.2$ Hz, 1H, NH_2), 7.60 (s, 1H, Ar–H), 7.49 (dd, $J = 8.5$, 2.2 Hz, 1H, Ar–H), 7.40 (d, $J = 8.3$ Hz, 1H, Ar–H), 7.34–7.26 (m, 2H, Ar–H), 7.24–7.20 (m, 2H, Ar–H), 7.06 (t, $J = 8.7$ Hz, 2H, Ar–H), 6.92 (dd, $J = 9.0$, 4.1 Hz, 2H, Ar–H), 5.72 (s, 1H, CH), 2.72 (t, $J = 7.1$ Hz, 2H, CH_2), 2.52–2.50 (m, 2H, CH_2), 2.28 (s, 3H, CH_3). ^{13}C NMR (126 MHz, DMSO-d_6) δ 159.52, 158.35, 157.61, 157.30, 152.66, 148.49, 148.21, 139.35, 135.37, 133.78, 132.42, 131.34, 130.27, 129.14, 128.80, 126.72, 118.03, 116.84, 116.65, 105.90, 56.48, 55.44, 41.88, 35.63, 19.03, 13.86. MS (MALDI-TOF) *m/z* 552 (M + 1).

6-(1-(2,4-Dichlorophenyl)-3-methyl-5-(p-tolyloxy)-1H-pyrazol-4-yl)-N^2-phenethyl-3-,6-dihydro-1,3,5-triazine-2,4-diamine (10h) White solid, Yield 42%; m.p. 88–90 °C. ^{1}H NMR (300 MHz, DMSO-d_6) δ 8.79 (s, 1H, NH), 8.50 (s, 1H, NH), 7.81 (d, $J = 2.2$ Hz, 1H, NH_2), 7.48 (dd, $J = 8.5$, 2.3 Hz, 1H, Ar–H), 7.38 (d, $J = 8.6$ Hz, 1H, Ar–H), 7.34–7.27 (m, 2H, Ar–H), 7.22 (t, $J = 5.3$ Hz, 3H, Ar–H), 7.03 (d, $J = 8.4$ Hz, 2H, Ar–H), 6.77 (d, $J = 7.8$ Hz, 2H, Ar–H), 5.66 (s, 1H, CH), 2.72 (d, $J = 6.5$ Hz, 2H, CH_2), 2.51 (d, $J = 1.8$ Hz, 2H, CH_2), 2.28 (s, 3H, CH_3), 2.20 (d, $J = 9.2$ Hz, 3H, CH_3). ^{13}C NMR (126 MHz, DMSO-d_6) δ 158.45, 157.41, 154.53, 149.06, 148.49, 148.36, 139.37, 135.23, 133.89, 133.23, 132.36, 131.25, 130.59, 130.27, 129.14, 128.76, 126.71, 115.90, 105.63, 55.46, 41.88, 35.62, 22.33, 20.57, 19.03, 13.96. MS (MALDI-TOF) *m/z* 548 (M + 1).

6-(1-(2,4-Dichlorophenyl)-5-(2,4-dimethylphenoxy)-3-methyl-1H-pyrazol-4-yl)-N^2-phenethyl-3,6-dihydro-1,3,5-triazine-2,4-diamine (10i) White solid, Yield 42%; m.p. 108–110 °C. ^{1}H NMR (300 MHz, DMSO-d_6) δ 8.77 (s, 1H, NH), 8.66 (s, 1H, NH), 8.51 (s, 1H, NH_2), 7.81 (d, $J = 2.2$ Hz, 2H, NH_2 and Ar–H), 7.46 (dd, $J = 8.5$, 2.3 Hz, 2H, Ar–H), 7.36 (s, 1H, Ar–H), 7.31 (dd, $J = 13.1$, 5.9 Hz, 3H, Ar–H), 7.21 (t, $J = 6.5$ Hz, 3H, Ar–H), 6.89 (s, 1H, Ar–H), 6.84 (d, $J = 8.4$ Hz, 1H, Ar–H), 6.61 (d, $J = 8.4$ Hz, 1H, Ar–H), 5.68 (s, 1H, CH), 2.69 (s, 2H, CH_2), 2.51–2.50 (m, 2H, CH_2), 2.29 (s, 3H, CH_3), 2.14 (s, 3H, CH_3), 2.05 (s, 3H, CH_3). ^{13}C NMR (126 MHz, DMSO-d_6) δ 158.38, 157.29, 152.91, 148.36, 139.34, 135.20, 133.83, 132.71, 132.23, 131.92, 131.75, 131.18, 130.20, 129.10, 128.72, 127.84, 126.71, 125.93, 114.12, 106.13, 56.48, 55.44, 41.86, 35.57, 22.41, 20.52, 19.02, 15.76, 13.88. MS (MALDI-TOF) *m/z* 562 (M + 1).

6-(1-(2,4-Dichlorophenyl)-3-methyl-5-(3-(trifluoromethyl)phenoxy)-1H-pyrazol-4-yl)-N^2-phenethyl-3,6-dihydro-1,3,5-triazine-2,4-diamine (10j) White solid, Yield 40%; m.p. 86–88 °C. ^{1}H NMR (300 MHz, DMSO-d_6) δ 8.91 (s, 1H, NH), 8.66 (s, 1H, NH), 7.86 (s, 1H, NH_2), 7.78 (d, $J = 2.2$ Hz, 1H, Ar–H), 7.63 (s, 1H, Ar–H), 7.47 (dd, $J = 13.0$, 4.5 Hz, 2H, Ar–H), 7.41 (d, $J = 7.3$ Hz, 2H, Ar–H), 7.33–7.25 (m, 2H, Ar–H), 7.21 (dd, $J = 9.7$, 4.5 Hz, 3H, Ar–H), 7.12 (s, 1H, Ar–H), 5.81 (s, 1H, CH), 2.68 (s, 2H, CH_2), 2.51–2.50 (m, 2H, CH_2), 2.31 (s, 3H, CH_3). ^{13}C NMR (126 MHz, DMSO-d_6) δ 158.28, 157.22, 156.43, 148.54, 147.29, 139.31, 135.47, 133.56, 132.31, 131.72, 131.26, 130.93, 130.68, 130.30, 129.10, 128.79, 126.71, 124.95, 122.78, 121.15, 120.55, 113.42, 106.66, 56.48, 55.38, 41.84, 35.58, 22.47, 19.02, 13.79. MS (MALDI-TOF) *m/z* 602 (M + 1).

6-(1-(2,4-Dichlorophenyl)-3-methyl-5-(naphthalen-2-yloxy)-1H-pyrazol-4-yl)-N^2-phenethyl-3,6-dihydro-1,3,5-triazine-2,4-diamine (10k) Yellow solid, Yield 38%; m.p. 116–118 °C. ^{1}H NMR (300 MHz, DMSO-d_6) δ 8.83 (s, 1H, NH), 8.73 (s, 1H, NH), 8.49 (s, 1H, NH_2), 8.09 (s, 1H, NH_2), 7.87 (d, $J = 8.5$ Hz, 1H, Ar–H), 7.76 (s, 1H, Ar–H), 7.67 (d, $J = 2.0$ Hz, 1H, Ar–H), 7.61–7.50 (m, 3H, Ar–H), 7.42 (d, $J = 8.2$ Hz, 1H, Ar–H), 7.33–7.24 (m, 4H, Ar–H), 7.20 (d, $J = 6.9$ Hz, 1H, Ar–H), 7.14 (s, 2H, Ar–H), 6.86 (d, $J = 7.6$ Hz, 1H, Ar–H), 5.79 (s, 1H, CH), 3.21 (s, 2H, CH_2), 2.57 (s, 2H, CH_2), 2.34 (s, 3H, CH_3). ^{13}C NMR (126 MHz, DMSO-d_6) δ 158.23, 157.20, 152.40, 147.97, 139.25, 135.12, 134.40, 133.67, 132.29, 131.19, 130.13, 129.05, 128.75, 128.57, 127.97, 127.36, 126.66, 126.18, 124.17, 123.76, 121.15, 109.39, 56.49, 55.44, 41.73, 35.39, 21.97, 19.02, 13.88. MS (MALDI-TOF) *m/z* 584 (M + 1).

In vitro inhibition of bacterial and fungal growth

Determination of minimal inhibitory concentrations (MICs) was performed as described previously [16]. The microorganisms used in the present study were *S. aureus* 4220, *E. Coli* 1924, *S. mutans* 3289, *P. aeruginosa* 2742, *S. typhimurium* 2421 and *C. albicans* 7535. The strains of multidrug-resistant clinical isolates were methicillin-resistant *S. aureus* (MRSA CCARM 3506) and quinolone-resistant *S. aureus* (QRSA CCARM 3505). Clinical isolates were collected from various patients hospitalized in several clinics. Test bacteria were grown to mid-log phase in Mueller–Hinton broth (MHB) and diluted 1000-fold in the same medium. The bacteria of 10^5 CFU/mL were inoculated into MHB and dispensed at 0.2 mL/well in a 96-well microtiter plate. As positive controls, oxacillin and norfloxacin were used. Test compounds were prepared in DMSO, the final concentration of which did not exceed 0.05%. A twofold serial dilution technique was used to obtain final concentrations of 64–0.25 µg/mL. The MIC was defined as the concentration of a test compound that completely inhibited bacteria growth during 24 h incubation at 37 °C. Bacteria growth was determined by measuring the absorption at 650 nm using

a microtiter enzyme-linked immunosorbent assay (ELISA) reader. All experiments were carried out three times.

Cytotoxicity assessment by MTT assay

The cytotoxicity test of selected compounds was measured through the colorimetric MTT assay. Human cancer cell lines MCF-7 and HeLa were bought from the Cell Bank of Chinese Academy of Sciences (Shanghai, China). MCF-7 and HeLa were grown in the Dulbecco's modification of eagle's medium (DMEM), (Corning) supplemented with 10% fetal bovine serum (FBS). A variety of concentrations of the test compounds (200, 100, 50, 25, 12.5, 6.25, 3.125, 1.625 μmol/L) dissolved by 10% distilled DMSO was added to each well. After incubation for 24 h at 37 °C under 5% CO_2, 2.5 μg/mL of MTT solution was added to each well. Further the plate was incubated for 4 h. Then, the medium was removed and the resulting formazan crystals were dissolved with 100 μL DMSO. After shaking 10 min, the optical density was measured at 570 nm using a microtiter ELISA reader. The selected compounds were used as positive control, whereas untreated cells were used as negative controls. The IC_{50} values were defined as the concentrations inhibiting 50% of cell growth. All experiments were performed in triplicate.

Molecular docking

Molecular docking protocol was followed according to the reported method [21, 22]. All docking runs were performed using the Discovery Studio (DS) 2017 software. The crystal structure data (*S. aureus* DHFR) were obtained from the Protein Data Bank (PDB ID: 3fra). The protein and ligand samples were prepared, water molecules were deleted, and a DS server added hydrogen. The docking result was treated with DS Client. The output poses of the ligands generated were analyzed using the LibDockScore function to find out the best complimentary match between the ligand and the receptor.

DHFR inhibition assay

The test of compounds **10d** and standard drug (**trimethoprim**) was measured through the ELISA assay. Solid-phase antibody was prepared by coating the microtiter plate wells with purified human dihydrofolate reductase (DHFR) antibody. A variety of concentrations of the test compound (0, 0.1, 0.3, 1, 3, 10 μmol/L) was combined with DHFR. After incubation for 1.5 h at 37 °C, HRP labeled was added. After washing completely, TMB substrate was added, and TMB substrate was becoming blue color at HRP enzyme-catalyzed. Reaction was terminated by the addition of a sulfuric acid solution, and the color change was measured spectrophotometrically at a wavelength of 450 nm. The concentration of DHFR activity was calculated by a standard curve.

Acknowledgements This work was supported by the National Natural Science Foundation of China (No. 81773692); the Science and Technology Department of Jilin Province (No. 20180311016YY), the Department of Education of Jilin Province (No. JJKH20191070KJ); the Health Department of Jilin Province (No. 2018ZC034); and the Doctoral Foundation of Jilin Medical University (No. JYBS2018007).

Compliance with ethical standards

Conflict of interest The authors state no conflict of interest.

References

1. Pasero C, D'Agostino I, De Luca F, Zamperini C, Deodato D, Truglio GI, Sannio F, Del Prete R, Ferraro T, Visaggio D, Mancini A, Guglielmi MB, Visca P, Docquier JD, Botta M (2018) Alkyl-guanidine compounds as potent broad-spectrum antibacterial agents: chemical library extension and biological characterization. J Med Chem 61:9162–9176. https://doi.org/10.1021/acs.jmedchem.8b00619
2. https://www.cdc.gov/drugresistance/index.html
3. Overbye KM, Barrett JF (2005) Antibiotics: where did we go wrong? Drug Discov Today 10:45–52. https://doi.org/10.1016/S1359-6446(04)03285-4
4. Yin Z, Whittell LR, Wang Y, Jergic S, Liu M, Harry EJ, Dixon NE, Beck JL, Kelso MJ, Oakley AJ (2014) Discovery of lead compounds targeting the bacterial sliding clamp using a fragment-based approach. J Med Chem 57:2799–2806. https://doi.org/10.1021/jm500122r
5. Tanitame A, Oyamada Y, Ofuji K, Fujimoto M, Iwai N, Hiyama Y, Suzuki K, Ito H, Kawasaki M, Nagai K, Wachi M, Yamagishi J (2004) Synthesis and antibacterial activity of a novel series of potent DNA gyrase inhibitors. Pyrazole derivatives. J Med Chem 47:3693–3696. https://doi.org/10.1021/jm030394f
6. Güniz KS, Rollas S, Erdeniz H, Kiraz M, Cevdet EA, Vidin A (2000) Synthesis, characterization and pharmacological properties of some 4-arylhydrazono-2-pyrazoline-5-one derivatives obtained from heterocyclic amines. Eur J Med Chem 35:761–771. https://doi.org/10.1016/s0223-5234(00)90179-x
7. Penning TD, Talley JJ, Bertenshaw SR, Carter JS, Collins PW, Docter S, Graneto MJ, Lee LF, Malecha JW, Miyashiro JM, Rogers RS, Rogier DJ, Yu SS, Anderson GD, Burton EG, Cogburn JN, Gregory SA, Koboldt CM, Perkins WE, Seibert K, Veenhuizen AW, Zhang YY, Isakson PC (1997) Synthesis and biological evaluation of the 1,5-diarylpyrazole class of cyclooxygenase-2 inhibitors: identification of 4-[5-(4-methylphenyl)-3- (trifluoromethyl)-1H-pyrazol-1-yl]benzenesulfonamide (SC-58635, Celecoxib). J Med Chem 40:1347–1365. https://doi.org/10.1021/jm960803q
8. Sridhar R, Perumal PT, Etti S, Shanmugam G, Ponnuswamy MN, Prabavathy VR, Mathivanan N (2004) Design, synthesis and antimicrobial activity of 1*H*-pyrazole carboxylates. Bioorg Med Chem Lett 14:6035–6040. https://doi.org/10.1016/j.bmcl.2004.09.066
9. Comber RN, Gray RJ, Secrist JA (1992) Acyclic analogues of pyrazofurin: syntheses and antiviral evaluation. Carbohydr Res 216:441–452. https://doi.org/10.1016/0008-6215(92)84179-v
10. Kompis IM, Islam K, Then RL (2005) DNA and RNA synthesis: antifolates. Chem Rev 105:593–620. https://doi.org/10.1021/cr0301144

11. Wright DL, Anderson AC (2011) Antifolate agents: a patent review (2006–2010). Expert Opin Ther Pat 21:1293–1308. https://doi.org/10.1517/13543776.2011.587804
12. Hawser S, Lociuro S, Islam K (2006) Dihydrofolate reductase inhibitors as anti-bacterial agents. Biochem Pharmacol 71:941–948. https://doi.org/10.1016/j.bcp.2005.10.052
13. Zheng CJ, Song MX, Sun LP, Wu Y, Hong L, Piao HR (2012) Synthesis and biological evaluation of 5-aryloxypyrazole derivatives bearing a rhodanine-3-aromatic acid as potential antimicrobial agents. Bioorg Med Chem Lett 22:7024–7028. https://doi.org/10.1016/j.bmcl.2012.09.107
14. Xu LL, Zheng CJ, Sun LP, Miao J, Piao HR (2012) Synthesis of novel 1,3-diaryl pyrazole derivatives bearing rhodanine-3-fatty acid moieties as potential antibacterial agents. Eur J Med Chem 48:174–178. https://doi.org/10.1016/j.ejmech.2011.12.011
15. Zhang TY, Zheng CJ, Wu J, Sun LP, Piao HR (2019) Synthesis of novel dihydrotriazine derivatives bearing 1,3-diaryl pyrazole moieties as potential antibacterial agents. Bioorg Med Chem Lett 29:1079–1084. https://doi.org/10.1016/j.bmcl.2019.02.033
16. Bai XQ, Chen Y, Liu Z, Zhang LH, Zhang TY, Feng B (2019) Synthesis, antimicrobial activities, and molecular docking studies of dihydrotriazine derivatives bearing a quinoline moiety. Chem Biodivers 16:e1900056. https://doi.org/10.1002/cbdv.201900056
17. Fang XF, Li D, Tangadanchu VKR, Gopala L, Gao WW, Zhou CH (2017) Novel potentially antifungal hybrids of 5-flucytosine and fluconazole: design, synthesis and bioactive evaluation. Bioorg Med Chem Lett 27:4964–4969. https://doi.org/10.1016/j.bmcl.2017.10.020
18. Gao WW, Rasheed S, Tangadanchu VKR, Sun Y, Peng XM, Cheng Y, Zhang FX, Lin JM, Zhou CH (2017) Design, synthesis and biological evaluation of amino organophosphorus imidazoles as a new type of potential antimicrobial agents. Sci China Chem 60:769–785. https://doi.org/10.1007/s11426-016-9009-6
19. Zapotoczna M, O'Neill E, O'Gara JP (2016) Untangling the diverse and redundant mechanisms of *Staphylococcus aureus* biofilm formation. PLoS Pathog 12:e1005671. https://doi.org/10.1371/journal.ppat.1005671
20. Soto SM (2013) Role of efflux pumps in the antibiotic resistance of bacteria embedded in a biofilm. Virulence 4:223–229. https://doi.org/10.4161/viru.23724
21. Lam T, Hilgers MT, Cunningham ML, Kwan BP, Nelson KJ (2014) Structure-based design of new dihydrofolate reductase antibacterial agents: 7-(benzimidazol-1-yl)-2,4-diaminoquinazolines. J Med Chem 57:651–668. https://doi.org/10.1021/jm401204g
22. Oefner C, Bandera M, Haldimann A, Laue H, Schulz H (2009) Increased hydrophobic interactions of iclaprim with *Staphylococcus aureus* dihydrofolate reductase are responsible for the increase in affinity and antibacterial activity. J Antimicrob Chemother 63:687–698. https://doi.org/10.1093/jac/dkp024